Pharmacological Inhibition of PHOSPHO1 Suppresses Vascular Smooth Muscle Cell Calcification

Published in final edited form as:
J Bone Miner Res. 2013 January ; 28(1): 81–91. doi:10.1002/jbmr.1733.

Pharmacological inhibition of PHOSPHO1 suppresses vascular smooth muscle cell calcification

Tina Kiffer-Moreira, Ph.D.[1], **Manisha C Yadav, Ph.D.**[1], **Dongxing Zhu, Ph.D.**[2], **Sonoko Narisawa, Ph.D.**[1], **Campbell Sheen, Ph.D.**[1], **Boguslaw Stec, Ph.D.**[1], **Nicholas D. Cosford, Ph.D.**[3], **Russell Dahl, Ph.D.**[3], **Colin Farquharson, Ph.D.**[2], **Marc. F. Hoylaerts, Ph.D.**[4], **Vicky E. MacRae, Ph.D.**[2], and **José Luis Millán, Ph.D.**[1]

[1]Sanford Children's Health Research Center, Sanford-Burnham Medical Research Institute, La Jolla, CA, USA

[2]The Roslin Institute, The University of Edinburgh, Easter Bush, Roslin, Midlothian, EH25 9RG, Scotland, UK

[3]Conrad Prebys Center for Chemical Genomics, Sanford-Burnham Medical Research Institute, La Jolla, CA 92037, USA

[4]Center for Molecular and Vascular Biology, University of Leuven, Leuven, Belgium

Abstract

Medial vascular calcification (MVC) is common in patients with chronic kidney disease, obesity, and aging. MVC is an actively regulated process that resembles skeletal mineralization, resulting from chondro-osteogenic transformation of vascular smooth muscle cells (VSMCs). Here, we used mineralizing murine VSMCs to study the expression of PHOSPHO1, a phosphatase that participates in the first step of matrix vesicles-mediated initiation of mineralization during endochondral ossification. Wild-type (WT) VSMCs cultured under calcifying conditions exhibited increased *Phospho1* gene expression and *Phospho1*$^{-/-}$ VSMCs failed to mineralize *in vitro*. Using natural PHOSPHO1 substrates, potent and specific inhibitors of PHOSPHO1 were identified via high-throughput screening and mechanistic analysis and two, designated MLS-0390838 and MLS-0263839, were selected for further analysis. Their effectiveness in preventing VSMC calcification by targeting PHOSPHO1 function was assessed, alone and in combination with a potent tissue-nonspecific alkaline phosphatase (TNAP) inhibitor MLS-0038949. PHOSPHO1 inhibition by MLS-0263839 in mineralizing WT cells (cultured with added inorganic phosphate) reduced calcification in culture to 41.8% ± 2.0 of control. Combined inhibition of PHOSPHO1 by MLS-0263839 and TNAP by MLS-0038949 significantly reduced calcification to 20.9% ± 0.74 of control. Furthermore, the dual inhibition strategy affected the expression of several mineralization-related enzymes while increasing expression of the smooth muscle cell marker *Acta2*. We conclude that PHOSPHO1 plays a critical role in VSMC mineralization and that "phosphatase inhibition" may be a useful therapeutic strategy to reduce MVC.

Address for correspondence: José Luis Millán, Ph. D., Sanford Children's Health Research Center, Sanford-Burnham Medical Research Institute, 10901 North Torrey Pines Road, La Jolla, CA 92037, Tel: 858-646-3130, FAX: (858) 795-5298, millan@sanfordburnham.org.

Disclosure
All the authors state that they have no conflicts of interest.

Keywords

High-throughput screening; small-molecules; pharmacological inhibitors; alkaline phosphatase; kinetic studies

INTRODUCTION

Medial vascular calcification (MVC), also known as Monckeberg's sclerosis, is characterized by the deposition of hydroxyapatite (HA) crystals within the medial layers of arteries and is increasingly recognized as an important clinical problem.[1,2] For decades, calcification of the cardiovascular system was considered an uncommon condition limited to advanced senile arteriosclerosis. However, its prevalence corresponds roughly with age, with coronary artery calcification occurring in 20% of young adults, 60% in the middle age group, and 90% of the elderly.[3] Although vascular calcification is a major contributor to cardiovascular disease (CVD) and death in patients with chronic kidney disease (CKD), there is no established treatment for this morbid condition.[4,5]

MVC follows an active endochondral ossification-like process, resulting in the formation of bone marrow and cartilage.[6,7] The process involves chondro-osteoblastic conversion of vascular smooth muscle cells (VSMCs),[8,9] evident from the loss of characteristic smooth muscle cell markers and development of osteoblastic features, such as expression of tissue-nonspecific alkaline phosphatase (TNAP), osteocalcin (BGLAP) and osteopontin (SPP1), and osteocyte markers such as sclerostin and podoplanin.[10-14] It has been hypothesized that phosphate accelerates this chondro-osteogenic conversion by inducing expression of runt-related transcription factor 2 (RUNX2), osteocalcin and TNAP.[15] Elevated TNAP further favors vascular calcification by hydrolyzing the calcification suppressor inorganic pyrophosphate (PP_i).[16-19] The importance of PP_i has been illustrated in mouse models, deficient in ectonucleotide pyrophosphatase/phosphodiesterase 1 (*Enpp1*$^{-/-}$), or in the PP_i-channeling function of ANK (*ank/ank*). Both models are characterized by decreased levels of extracellular PP_i, caused by a combination of deficient output and increased degradation by TNAP, and exhibit a phenotype of hypermineralization.[20] We have shown in *Enpp1*$^{-/-}$ mouse that inhibition of TNAP by potent inhibitors can restore PP_i to sufficient levels to maintain normal mineralization.[16]

The phosphatase PHOSPHO1, first identified in the chicken as a member of the haloacid dehalogenase superfamily of Mg^{2+}-dependent hydrolases,[21-24] is expressed in chondrocytes in mineralizing cartilage at levels 120-fold higher than in non-mineralizing tissues.[25] PHOSPHO1 shows high phosphohydrolase activity towards phosphoethanolamine (P-Etn) and phosphocholine (P-Cho), both of which are key components of matrix vesicles' (MVs) phospholipids.[26] Using lansoprazole as a pharmacological inhibitor of PHOSPHO1, we demonstrated that PHOSPHO1 is present and active inside chondrocyte- and osteoblast-derived MVs.[25] However, lansoprazole was identified from the Library of Pharmacologically Active Compounds (LOPAC^{1280}) and, as expected, inhibits a number of proteins other than PHOSPHO1, including TNAP.[27,28] More recently, we showed that PHOSPHO1 and TNAP expression coincide during skeletal mineralization[29] and using single and double knockout mice, we demonstrated that PHOSPHO1 controls TNAP expression in mineralizing cells and is essential for mechanically competent mineralization.[30,31] Furthermore, PHOSPHO1/TNAP double knockout mice show complete absence of skeletal mineralization.[30]

Ultrastructural studies have identified HA-containing MVs in human aorta, which indicates that these structures may provide the nidus for vascular calcification.[32,33] In this study, we

provide the first description of the role of PHOSPHO1 in the calcification of VSMCs. We show that inhibition of PHOSPHO1 activity can reduce calcification in hypermineralizing wild-type (WT) VSMCs and that the combined use of selective PHOSPHO1 and TNAP inhibitors considerably reduces calcification in these cells, indicating that "phosphatase inhibition" constitutes a viable approach for the prevention and treatment of MVC.

MATERIALS and METHODS

Isolation and culture of primary WT, *Phospho1*$^{-/-}$ and *Enpp1*$^{-/-}$ VSMCs

Vascular smooth muscle cells (VSMCs) isolated from WT, *Enpp1*$^{-/-}$ and *Phospho1*$^{-/-}$ mice were used for *in vitro* calcification studies. The VSMCs were isolated from excised aortas using a collagenase digestion method and the smooth muscle phenotype was confirmed by RT-PCR analysis for smooth muscle α-actin as before.[16] One mouse aorta provided an average of 5×10^5 VSMCs. These cells were cultured (in triplicate) at a density of 0.25×10^5 cells/mL/well in a 24 well plate using α-MEM supplemented with 50 μg/mL ascorbic acid and 2.5 mmol/L β-glycerophosphate or 3 mmol/L sodium phosphate to induce calcification. Cells were cultivated in the mineralization media for up to four weeks and media was changed every second day. Inhibitors were freshly dissolved in dimethylsufoxide (DMSO) and added at each medium change at a final concentration of 30 μmol/L.

Analysis of gene expression

RNA was extracted using an RNAeasy Plus Kit (Qiagen, Valencia, CA, USA), according to the manufacturer's instructions. RNA was reverse transcribed and specific cDNAs were quantified by real-time PCR using dual-labeled hydrolysis probes (FAM-TAMRA) as before.[14,30] Primers and probes were obtained from Eurogentec North America (San Diego, CA, USA) and their sequences are provided in the Data Supplement.

Expression and preparation of test enzymes

A construct for expression of the human bone-specific PHOSPHO1 isoform was generated by ligating a PCR fragment encoding the bone specific N-terminal 40 amino acids, a partial fragment of cDNA (Genebank accession BC117187) encoding the common isoform, and a C-terminal polyhistidine tag into the pCMV-SCRIPT vector. The expression vector was transfected into HEK293 cells, and recombinant bone isoform PHOSPHO1 protein was purified by a standard procedure.[26] Soluble epitope-tagged human TNAP and ENPP1 was produced and purified as described previously.[16]

High-throughput screening

High-throughput screening (HTS) of 55,000 compounds from the MLSMR compound collection was conducted using a colorimetric assay based on the ability of PHOSPHO1 to liberate phosphate from P-Etn and its reaction with the Biomol Green reagent (Biomol International, Plymouth Meeting, PA, USA). HTS provided approximately 5,000 compounds that showed greater than 50% activity in the single point assay, a hit rate of 3%. Subsequent hit follow up and validation in dose response identified sub-micromolar inhibitors of PHOSPHO1 (see PubChem BioAssay AID 1666 for details). Initial HTS was performed in duplicate at a concentration of 20 μmol/L with dose-response assays using a 10-point two-fold serial dilution of the hit compounds in DMSO. Hit confirmation was performed using the Biomol Green colorimetric assay to verify inhibitory activity against PHOSPHO1 in dose-response mode. Compounds that were active in dose-response mode against PHOSPHO1 and soluble in the range relevant to their potency were prioritized for synthetic chemistry follow-up to increase selectivity against ENPP1 and TNAP and/or potency against PHOSPHO1.

Enzyme kinetics

Reactions were measured in triplicate in 96-well plates containing 20 mmol/L MES-NaOH, pH 6.7, 0.01% (w/v) BSA, 0.0125% (v/v) Tween-20, 2 mmol/L $MgCl_2$, 62.5 μmol/L P-Etn or P- Cho (Sigma-Aldrich, St. Louis, MO, USA), test compound dissolved in DMSO (ranging from 0.0143 nmol/L - 300 μmol/L) and 0.3 nmol/L of purified recombinant human PHOSPHO1, in a total volume of 50 μL. Each reaction contained a final concentration of 1% (v/v) DMSO, which was determined to be insufficient to interfere with PHOSPHO1 activity (data not shown). Enzyme was pre-incubated with the inhibitors and the reaction was initiated by addition of substrate 1,2-dioleoyl-sn-glycero-3-phosphoethanolamine (Sigma-Adrich, P-Eth) or phosphocholine chloride calcium salt tetrahydrate (Sigma-Aldrich, P-Chol) and allowed to proceed for 60 min at room temperature. Reactions were stopped with 100 μL Biomol Green reagent and absorbance was measured at 620 nm, after which the inhibitory effect of each compound was calculated as a percentage of control. The IC_{50} was calculated from plots of residual enzyme activity against inhibitor concentration, using Origin Scientific plotting software (Northampton, MA, USA). Single point experiments with inhibitors at 30 μmol/L were performed to test selectivity for PHOSPHO1 inhibition versus TNAP inhibition, at those concentrations used during VSMC calcification, as described previously.[16]

The inhibition of recombinant human TNAP, and three TNAP variants (Tyr371Ala, Glu108Phe and His434Glu), with mutations previously implicated in the active site positioning of the classic TNAP inhibitor levamisole,[34] by the TNAP inhibitor MLS-0038949[35] was carried out at pH 7.5, as previously reported.[16] The nature of the inhibition was investigated using double reciprocal plots of velocity (v) versus substrate concentration, at various inhibitor concentrations (0-1 μmol/L) and secondary replots. Likewise, the nature of the inhibition of PHOSPHO1 by the selected inhibitors was determined via double reciprocal plots of v versus the concentration of P-Etn.

Computer modeling and docking

To complement the kinetic studies on PHOSPHO1 inhibition by both classical inhibitors such a lansoprazole[25] and the novel inhibitors described here, we modeled the protein and performed computer docking. Several protein models were obtained using a number of homology modeling web servers. The PHOSPHO1 protein sequence was extracted from the NCBI Protein database and submitted for homology modeling using FFAS03,[36] ITASSER,[37] and SWISSModel.[38] Retrieved models were superposed and regions of high structural homology (consensus structure) were defined. The mobile regions were examined and the models were grouped into conformational classes as judged by the RMSD. The models showed divergence in two areas: two helices and two loops closing the active site. Structural representatives of at least three classes of models were extracted and used for docking using the SwissDock server[39] and the program EAdock.[40] A single model of PHOSPHO1, produced by ITASSER, was selected as all other classes had hindered access to the active site. Docking was performed using this model with selected PHOSPHO1 inhibitors. One hundred and fifty hits with the highest pseudo-energy were retained in the search. Subsequently, clustering analysis was performed and the hits were clustered into spatially matching hits. The representatives of these families show different binding modes for individual compounds.

Calcification assay

Calcium deposition in cultured VSMCs in the presence or absence of inhibitors was evaluated by staining cell layers with Alizarin Red, as before.[16] Cells were washed twice with both PBS and 70% ethanol, then fixed in 100% ethanol for 5 min. Cells were stained with 2% Alizarin Red (pH 4.2) for 30 min at room temperature and washed with distilled

water. Alizarin Red-stained cultures were extracted with 10% cetylpyridium chloride for 45 min and $A_{570\ nm}$ was measured. The matrix was also decalcified in 0.6 N HCl for 24 hours, and free calcium was determined colorimetrically using a commercially available kit (Randox Laboratories, Crumlin, UK), after correction for total protein concentration. The protein content of the cultures was measured using Bio-Rad protein assay reagent (Bio-Rad Laboratories, Hertfordshire, UK) based on the Bradford dye procedure, and gamma globulin was used as a standard (Fig.1 C, D). For experiments of effect of inhibitors on mineralization of cultured WT, *Enpp1*$^{-/-}$ and *Phospho1*$^{-/-}$ VSMCs the cell layers were stained with Alizarin Red, extracted with 10% cetylpyridium and A_{570} was measured.

MTT reduction assay for cell viability

Cells were cultivated for 7 days and treated with 30 μmol/L of TNAP and/or PHOSPHO1 inhibitors as described previously. To determine cell viability, the growth medium was removed and cells were incubated with 3-(4,5-dimethyl-2-thiazolyl)-2,5-diphenyl-2H-tetrazolium bromide (MTT, Sigma-Aldrich) at a final concentration of 0.5 mg/mL in phenol-red-free DMEM containing 10% heat-inactivated FBS at 37°C in the dark for 3.5 hours. An equal volume of the dissolving buffer (22% (w/v) SDS in 0.02 M HCl) was added to the wells with gentle trituration. Cultures were incubated with the dissolving buffer at 37°C in the dark for 4 hours. After the dye was completely dissolved, 200 μL of the solution was transferred to a 96-well plate and absorbance was recorded at 570 nm.

Statistical analysis

All data are expressed as the mean ± S.E.M. Differences in relative RNA expression for *Phospho1* and *Alpl* in WT VSMCs and for calcium deposition in *Phospho1*$^{-/-}$ versus WT VSMCs were analyzed with an unpaired t test with Welch correction and calculation of a two-tailed p value. Differences in the degree of VSMC calcification and multiple comparisons of the relative RNA expression data were also analyzed by Student's *t* test. The upregulation of *Phospho1* in VSMCs and osteoblasts was analyzed as a function of time by linear regression analysis. P values less than 0.05 were considered significant. Statistical tests were performed using Instat 3 (GraphPad, San Diego, CA, USA).

RESULTS

Role of PHOSPHO1 in VSMCs calcification

Phospho1 mRNA expression was measured in WT VSMC cultures, under calcifying conditions over 28 days and compared to *Phospho1* expression in WT calvarial osteoblasts. In osteoblasts, the normalized *Phospho1* expression increased in a linear manner (r^2=0.9, p <0.0001) until day 28 (Fig. 1A). In VSMCs, *Phospho1* expression was upregulated and increased linearly (r^2 = 0.881, p <0.0001) until day 21, then plateaued between days 21 and 28 (Fig. 1B). To confirm that PHOSPHO1 is a key enzyme in VSMC mineralization, we analyzed calcium deposition normalized to the amount of protein in 28 day cultured *Phospho1*$^{-/-}$ VSMCs, in comparison to WT control cells. Quantitative (Fig. 1C) and qualitative (Fig. 1D) analyses of calcium deposition indicated a reduced ability of *Phospho1*$^{-/-}$ VSMCs to calcify. We also examined the expression of *Phospho1* and *Alpl* mRNA in *Enpp1*$^{-/-}$ VSMCs. The initial *18s*-normalized *Alpl* expression was approximately 10-fold higher in *Enpp1*$^{-/-}$ VSMCs than in WT after 21 days of culture, in agreement with our previous observations,[16] while *Phospho1* expression in *Enpp1*$^{-/-}$ VSMCs was slightly lower than in WT VSMCs (Fig. 1E).

Selection and properties of PHOSPHO1 and TNAP inhibitors

Because PHOSPHO1 is upregulated in cultures of calcifying WT VSMCs and the known PHOSPHO1 inhibitor lansoprazole lacks target specificity, development of more specific PHOSPHO1 inhibitors is necessary to study the effect of PHOSPHO1 inhibition in VSMC calcification. High throughput screening for PHOSPHO1 inhibitors revealed several potent hits in the benzoisothiazolone class of compounds, indicating a nascent structure-activity-relationship (SAR) that would provide traction for inhibitor optimization. The potency and selectivity of the synthesized compounds were assessed by *in vitro* enzymatic assays using purified human PHOSPHO1, TNAP[42] and ENPP1 (see Data Supplement Fig. S1 for the dose-response curves for the inhibition of PHOSPHO1 by the nine new inhibitors using PHOSPHO1 natural substrates P-Etn and P-Cho). The IC_{50} values derived from these plots are shown in Table 1. MLS-0390838 and MLS-0263839 were the most potent, with IC_{50} values of 0.13 and 0.14 μmol/L respectively.The mechanism of PHOSPHO1 inhibition was investigated via double reciprocal plots of PHOSPHO1 activity versus substrate concentration (32-170 μmol/L), in the presence of various concentrations of inhibitor (0-0.9 μmol/L). Fig. 2 shows how these lines intersect on the y-axis, confirming the competitive nature of the inhibition for both lansoprazole (Fig. 2A) and MLS-0263839 (Fig. 2B) with K_i values of 0.16 ± 0.03 μmol/L and 0.22 ± 0.01 μmol/L, respectively. Likewise, MLS-0390838 was found to inhibit PHOSPHO1 in a competitive manner (not shown). MLS-0390838 and MLS-0263839 were selected as specific PHOSPHO1 inhibitors, as they showed minimal cross-inhibition of TNAP (Fig. 3A, B) and no inhibition of ENPP1 activity (not shown). Figure 3C, D show the specific inhibition of PHOSPHO1 by MLS-0390838 and MLS-0263839 using P-Etn (Fig. 3C) and P-Chol (Fig. D) as substrates.

Inhibition of TNAP has been shown to prevent VSMC calcification.[16] To achieve more potent TNAP inhibition, new inhibitors were identified.[35] In this study we aimed to determine whether combined inhibition of both TNAP and PHOSPHO1 was more effective than inhibition of either enzyme on its own. To accomplish this, we characterized the previously reported TNAP inhibitor MLS-0038949[35] to evaluate its suitability for inclusion in combined phosphatase inhibition experiments. MLS-0038949 was able to inhibit the p-nitrophenylphosphatase (Fig. 3A) (pNPPase) and pyrophosphatase (PP_iase) activities of TNAP (Fig. 3B). Conversely, Fig. 3C and D shows that this compound selectively inhibits TNAP, but not PHOSPHO1. We also studied the mechanism of TNAP inactivation by MLS-0038949 at pH 9.8 (not shown) and pH 7.5 (Fig. 4) as described before.[16] The parallel lines (Fig. 4A) indicate that TNAP is inhibited by MLS-0038949 in an uncompetitive manner, both at pH 7.5 and at pH 9.8 (not shown). Secondary re-plots of the y-axis intercepts allow derivation of the corresponding inhibition constant, which was calculated as K_i = 0.32 ± 0.04 μmol/L at pH 7.5 and 0.74 ± 0.01 μmol/L at pH 9.8. The active site positioning of MLS-0038949 (Fig. 4B) was investigated in inhibition studies with TNAP mutants implicated in the active site positioning of the classic TNAP inhibitor levamisole[36] (Glu108Phe, Tyr371Ala and His434Glu) and compared to inhibition by the reference compound levamisole (Fig. 4C). These analyses revealed that, similar to levamisole, MLS-0038949 positioning in the TNAP active site depends primarily on the active site residues Tyr371 and His434, which are important for TNAP function and for the stabilization of uncompetitive inhibitors levamisole and theophylline.[34] Correspondingly, the K_i values for the inhibition of TNAP by MLS-0038949 at pH 7.5 were 0.13 ± 0.02 μmol/L (Glu108Phe), 4.1 ± 0.5 μmol/L (Tyr371Ala), and 20 ± 1.7 μmol/L (His434Glu).

In silico docking of inhibitors in the active site

A model of PHOSPHO1 produced by ITASSER displayed the best features for molecular docking and was used for further studies. The model showed an organized tertiary structure with well-packed external helices surrounding the beta-pleated core of the protein. The

active site, identified by homology to mouse 5'-nucleotidase III (Protein Data Bank ID 2bdu) and phosphoserine phosphatase from *Helicobacter pylori* (Protein Data Bank ID 3m1y) was located deep in the protein matrix and was surrounded by two helices with two loops closing the site. The metal ion was modeled into the active site as suggested by the presence of homologous carboxylate bearing groups (Asp and Glu). Docking carried out in SwissDock with three compounds (lansoprazole, MLS-0263839, MLS-0390838) produced 150 top scoring hits for each. Clustering analysis identified 19 clusters (docking poses) for lansoprazole, 6 clusters for MLS-0263839 and 17 clusters for MLS-0390838. Analysis of all clusters showed different binding modes for individual compounds in reference to the three-dimensional location of the active site. Only a single cluster for lansoprazole and MLS-0390838 was not located in the active site pocket. The rest of the clusters were blocking the entry to the metal ion-binding pocket, although none of the compounds had a direct contact with a metal ion, consistent with the competitive nature of these inhibitors. For visualization purposes, a single representative of every compound with the best pseudo-energy score was selected. The pseudo-energy of these representatives corresponds with the physiological effect and affinity of the compounds to PHOSPHO1. The highest pseudo-energy was shown by MLS-0390838 (30 kcal/mol), followed by MLS-0263839 (25 kcal/mol) and lansoprazole (15 kcal/mol). Fig. 5A shows a comparison of docking poses for the lowest energy representatives of lansoprazole, MLS-0390838 and MLS-0263839 in the PHOSPHO1 active site. In this model MLS-0390838 and MLS-0263839 do not penetrate deeply into the active site pocket and do not interact with the catalytic site metal ion. Likewise, Fig. 5B shows MLS-0038949 docked in the TNAP active site. Docking of this uncompetitive TNAP inhibitor indicates a preferred interaction with active site residue His434, consistent with the kinetic data.

Inhibition of *in vitro* VSMC calcification and its effect in relative mRNA expression

The effect of the PHOSPHO1 and TNAP inhibitors on calcification of WT, *Enpp1*$^{-/-}$ and *Phospho1*$^{-/-}$ VSMCs was investigated. Toxicity of the inhibitors in 7 day cultures of WT VSMCs was excluded by MTT test (see Data Supplement Fig. S2). The MTT test was not successful in 21-day cultures because of the more extensive mineral content (not shown). Quantification of Alizarin Red staining of WT VSMCs cultivated for 21 days in the presence of inorganic phosphate (P_i) (Fig. 6A) or β-glycerophosphate (β-GP) (Fig. 6B) shows that MLS-0263839 was able to reduce mineralization to 41.8% ± 2.0 and 53.8% ± 4.1, respectively, relative to vehicle-treated control cells. The TNAP inhibitor (MLS-0038949) reduced Alizarin Red staining to54.4% ± 3.6 of the value for vehicle-treated WT VSMCs cultured in the presence of P_i and 62.1% ± 9.9 for WT VSMCs cultivated in the presence of β-GP, reinforcing the involvement of TNAP in vascular calcification [(16)]. Combined inhibition of both enzymes reduced calcification in P_i- and β-GP-containing media significantly further than inhibition of either inhibitor alone. Mineralization was reduced to 20.9% ± 0.74 (Fig. 6B) and 34.5% ± 0.78 (Fig. 6C) of the control by the MLS-0263839/MLS-0038949 combination in VSMCs cultured with P_i and β-GP, respectively. Lansoprazole alone and/or in combination with MLS-0038949 also significantly inhibited mineralization. The combination of the two PHOSPHO1 inhibitors, MLS-0026839 and lansoprazole was toxic to the cells (see Data Supplement Fig. S2). The effect of the inhibitors MLS-0038949, MLS-0263839 and combination MLS-0038949/MLS-0263839 were also investigated in *Enpp1*$^{-/-}$ and *Phospho1*$^{-/-}$ VSMCs. In *Enpp1*$^{-/-}$ VSMCs, both inhibitors strongly reduced mineralization and the combination MLS-0038949/MLS-0263839 essentially abolished *in vitro* mineralization in *Enpp1*$^{-/-}$ (Fig. 6C). As expected, in *Phospho1*$^{-/-}$ VSMCs, only the TNAP inhibitor MLS-0038949 significantly inhibited mineralization (Fig. 6D).

WT cells cultivated under the same conditions as described in Fig. 6B were analyzed for differences in the mRNA expression of key enzymes involved in mineralization as well as osteogenic and VSMC markers. Fig. 7 shows the effect of inhibitor treatment on the expression of osteogenic markers such as *Alpl*, *Runx2*, *Spp1*, *Bglap* and *Col1a1*. Fig. 7A shows that the combination of PHOSPHO1 and TNAP inhibitors significantly decreased the expression of *Alpl* mRNA ($p<0.05$) whereas the expression of *Enpp1* increased ($p<0.01$, Fig. 7B). The expression of *Phospho1* mRNA was not significantly different compared to the DMSO control cells in any of the treatments (Fig. 7C). Dual inhibitor treatment did not affect mRNA levels of the osteogenic markers *Runx2*, *Opn* and *Ocn* (Fig. 7D, E, F), but the expression of *Col1a1* was strongly decreased ($p<0.01$, Fig. 7G). In contrast, dual inhibition strongly raised expression of the VSMC marker *Acta2* (Fig. 7H).

DISCUSSION

The pathological mechanisms underlying medial vascular calcification are incompletely understood. It is known that MVC involves the loss of calcification suppressors, such as extracellular inorganic pyrophosphate (ePP_i).[43,44] We have shown previously that *Enpp1*$^{-/-}$ and *ank/ank* mice display equivalent reductions in plasma ePP_i concentrations[19,20] and both animal models develop comparable soft-tissue calcifications, including MVC accompanied by upregulation of TNAP expression in their VSMCs.[16] Furthermore, we have documented that MVC in the uremic rat, a model of end-stage renal disease, is accompanied by an increase in the expression of TNAP, a key enzyme in PP_i metabolism.[17] MVC resulting from NT5E deficiency also appears to be caused by elevated expression of TNAP.[45]

More recently, the role of another phosphatase, PHOSPHO1, in calcification has been established. This enzyme is crucial for initiation of skeletal mineralization [30] and mechanically competent mineralization [31], and is found inside MVs in calcifying tissues.[23,25] PHOSPHO1has been proposed to scavenge P_i from phospholipids inside the MV to generate a P_i/PP_i ratio conducive to calcification, whereas TNAP acts later in the mineralization process by restricting extracellular PP_i. *Phospho1*$^{-/-}$ mice display a distinct phenotype, with growth plate abnormalities, spontaneous fractures, bowed long bones, osteomalacia and scoliosis.[30] Consistent with the non-redundant functions of these two enzymes, transgenic over-expression of TNAP does not correct the bone phenotype in *Phospho1*$^{-/-}$ mice.[30] Furthermore, TNAP/PHOSPHO1 double knockout mice exhibit a phenotype more severe than those of the respective single knockouts: complete absence of skeletal mineralization. The importance of PHOSPHO1 in skeletal mineralization combined with the knowledge that MVC also appears to proceed via chondro-osteogenic differentiation of VSMCs and MV-mediated calcification [32,33], suggest that PHOSPHO1 might have a functional role in MVC and could serve as a therapeutic target. Here, we provide the first evidence that PHOSPHO1 is involved in MVC, as *Phospho1* expression increased in calcifying WT VSMCs and calcification was impaired in *Phospho1*$^{-/-}$ VSMCs.

Inhibitors of PHOSPHO1 identified from the small LOPAC^{1280} library of pharmacologically active compounds (lansoprazole, ebselen and SCH-202676), showed that inhibiting PHOSPHO1 function further impaired both the mineralization ability of MVs from TNAP null osteoblasts and skeletal mineralization of developing chick long bones.[25,29] Lansoprazole was previously reported to be specific for PHOSPHO1, but Ciancaglini *et al.* (2010) showed it partially inhibits ENPP1 and TNAP activity. [25,42] We also observed in the mineralization studies that lansoprazole showed toxicity to smooth muscle cells and that lansoprazole inhibited mineralization in *Phospho1*$^{-/-}$ chondrocytes (not shown), confirming its off-target effects. The HTS performed in this study provided two compounds (MLS-00390838 and MLS-0263839), superior to lansoprazole. These inhibitors

are highly selective for PHOSPHO1, with no detectable cross-inhibition of TNAP or ENPP1. MLS-00390838 and MLS-0263839 appeared to stabilize at several docking points inside the PHOSPHO1 active site, corroborating inhibitor selectivity. Both inhibitors act competitively, with sufficient affinity and selectivity to evaluate them as PHOSPHO1 inhibitors in VSMC calcification.

The finding that TNAP upregulation is a common phenomenon at sites of medial calcification in several disease models[16, 17, 45] has important translational implications and has motivated the development of potent inhibitors of the pyrophosphatase activity of TNAP to prevent and reverse MVC.[16, 35, 46-49] Selective inhibition of TNAP restores ePP_i concentrations to levels high enough to prevent aberrant mineralization[16,35,47]. To compare the relative merits of PHOSPHO1 and TNAP inhibition, we characterized the TNAP inhibitor, MLS-0038949, for use in mineralization assays. MLS-0038949 is highly specific for TNAP and does not cross-inhibit PHOSPHO1 or ENPP1.[35] MLS-0038949 is an uncompetitive TNAP inhibitor, stabilized in the active site by residues H434 and Y371.[17]

When VSMCs were cultured for 21 days in the presence of the PHOSPHO1 or TNAP inhibitors, PHOSPHO1 inhibition was more effective at preventing calcification than TNAP inhibition. This enhanced effect may be due to the earlier action of PHOSPHO1 that affects the intravesicular generation of HA seed crystals during MV-mediated calcification.[30] In addition, in complete agreement with the genetic data where ablation of *Phospho1* gene functions leads to dowregulation of *Alpl* gene expression,[30] we observe that the pharmacological inhibition of PHOSPHO1 leads to downregulation of *Alpl* mRNA. Thus, PHOSPHO1 appears to be a good target because not only is initiation of mineralization suppressed by the direct action of the inhibitor on PHOSPHO1 activity, but it also acts downstream by downregulating the amount of TNAP activity. Finally, the combined effect of both types of enzyme inhibitor suppressed VSMC calcification more than each inhibitor separately, both in WT and *Enpp1*$^{-/-}$ VSMCs. Interestingly, while double inhibition essentially abolished mineralization in *Enpp1*$^{-/-}$ VSMCs (by 93.2% ± 0.2, Fig. 6B), the effect was less pronounced in WT cells (65.5%± 0.7, Fig. 6C). This discrepancy may be accounted for by an increased *Enpp1* expression in WT cells, in response to double inhibition treatment (Fig. 7B), since it has been proposed that ENPP1 can act as a backup pyrophosphatase in the absence of TNAP and maintain the levels of calcification.[30] Thus, the enhanced inhibition seen in *Enpp1*$^{-/-}$ cells may be related to the absence of this compensatory mechanism. This effect was also observed by Villa-Bellosta *et al.*, using inhibitors in WT aortic ring cultures, [18] who found that TNAP inhibition reduced PP_i hydrolysis by approximately 50%,while the remaining hydrolysis was inhibited by the ENPP1 inhibitors α,β-methylene ATP and γ,β-α,β-methylene ATP.

MVC involves transdifferentiation of VSMCs into osteochondrogenic-like cells and consequent matrix mineralization. Here, we measured the effect of phosphatase inhibitors on the expression of various markers of these processes. We observed no significant difference in the expression of the osteochondrogenic markers *Runx2*, osteocalcin (*Bglap*) and osteopontin (*Spp1*) although expression of *Col1a1* was markedly impaired by the inhibitors, both alone and in combination. This indicates that phosphatase inhibition does not affect the chondro-osteogenic conversion of VSMCs, but prevents deposition of a matrix on which calcification can occur. While increased TNAP expression is also a marker of VSMC transdifferentiation, it was significantly downregulated in cultures containing the PHOSPHO1 inhibitor. This discrepancy can be explained by our previous work, which has shown that PHOSPHO1 knockout mice have reduced TNAP expression and activity. [30] MVC is also traditionally accompanied by loss of VSMC cell markers. Neither class of inhibitor alone affected expression of the VSMC gene *Acta2*, however it was significantly

higher in the combined inhibitor cultures, indicating that this treatment protected against loss of VSMCs features.

In conclusion, this paper shows that at least two phosphatases are implicated in VSMC calcification, and that combined phosphatase inhibition offers a promising approach for developing compounds to prevent or attenuate MVC. However, it is important to note that this strategy may interfere with normal bone formation both by interfering with the intravesicular initiation of HA seed crystal deposition mediated by PHOSPHO1 function as well as by interfering with extravesicular propagation of HA crystal deposition as a result of raising PP_i levels resulting from TNAP downregulation and inhibition and future work will need to address this potentially significant concern. Furthermore, study of selective inhibitors in cultured VSMCs also provides us with new insights about how the enzymes TNAP, PHOSPHO1 and ENPP1 interact during VSMC mineralization. We are currently using the scaffolds described here to design drug-like compounds for *in vivo* testing and further investigate the potential of PHOSPHO1 inhibitors as a potential treatment for MVC.

Supplementary Material

Refer to Web version on PubMed Central for supplementary material.

Acknowledgments

We wish to thank Soetkin Van Kerckhoven and Yalda Bravo for technical help. This work was supported in part by grant R01AR053102 and R01AR047908 from the National Institute of Arthritis and Musculoskeletal Diseases (NIAMS), and American Recovery and Reinvestment Act (ARRA) Challenge grant RC1HL10899 from the National Heart, Lung and Blood Institute (NHLB), National Institutes of Health (NIH), USA and Institute Strategic Program Grant Funding from the Biotechnology and Biological Sciences Research Council.

References

1. Chen NX, Moe SM. Arterial calcification in diabetes. Curr Diab Rep. 2003; 3:28–32. [PubMed: 12643143]
2. Doherty TMAK, Fitzpatrick LA, Wilkin DJ, Dtrano RC, Dunstan CR, Shah PK, Rajavashisth TB. Calcification in atherosclerosis: bone biology and chronic inflammation at the arterial crossroads. Proc Natl Acad Sci USA. 2003; 100:11201–11206. [PubMed: 14500910]
3. Towler DA, Demer LL. Thematic Series on the pathobiology of vascular calcification: an introduction. Circ Res. 2011; 108:1378–1380. [PubMed: 21617134]
4. van der Zee S, Baber U, Elmariah S, Winston J, Fuster V. Cardiovascular risk factors in patients with chronic kidney disease. Nat Rev Cardiol. 2009; 6:580–589. [PubMed: 19621012]
5. Jono S, Shioi A, Ikari Y, Nishizawa Y. Vascular calcification in chronic kidney disease. J Bone Miner Metab. 2006; 24:176–181. [PubMed: 16502129]
6. Lyemere VP, Proudfoot D, Weissberg PL, Shanahan CM. Vascular smooth muscle cell phenotypic plasticity and the regulation of vascular calcification. J Intern Med. 2006; 260:199–210.
7. Johnson K, Polewski M, van Etten D, Terkeltaub R. Chondrogenesis mediated by PPi depletion promotes spontaneous aortic calcification in NPP1–/– mice. Arterioscler Thromb Vasc Biol. 2005; 25:686–691. [PubMed: 15625282]
8. Tyson KL, Reynolds JL, McNair R, Zhang Q, Weissberg PL, Shanahan CM. Osteo/chondrogenic transcription factors and their target genes enhibit distinct patterns of expression in human arterial calcification. Arterioscler Thromb Vasc Bio. 2003; 23:489–494. [PubMed: 12615658]
9. Shanahan CM, Crouthamel MH, Kapustin A, Giachelli CM. Arterial calcification in chronic kidney disease: key roles for calcium and phosphate. Circ Res. 2011; 109:697–711. [PubMed: 21885837]
10. Qiao JH, Mertens RB, Fishbein MC, Geller SA. Cartilaginous metaplasia in calcified diabetic peripheral vascular disease: morphologic evidence of enchondral ossification. Hum Pathol. 2003; 34:402–407. [PubMed: 12733123]

11. Shroff RC, McNair R, Figg N, Skepper JN, Schurges L, Gupta A, Hiorns M, Donald AE, Deanfield J, Rees L, Shanaham CM. Dialysis accelerates medial vascular calcification in part by triggering smooth muscle cell apoptosis. Circulation. 2008; 118:1748–1757. [PubMed: 18838561]
12. El-Abbadi MM, Pai AS, Leaf EM, Yang HY, Bartley BA, Quan KK, Ingalls CM, Liao HW, Giachelli CM. Phosphate feeding induces arterial medial calcification in uremic mice: role of serum phosphorus, fibroblast growth factor-23, and osteopontin. Kidney Int. 2009; 75:1297–1307. [PubMed: 19322138]
13. Nakano-Kurimoto R, Ikeda K, Uraoka M, Nakagawa Y, Yutaka K, Koide M, Takahashi T, Matoba S, Yamada H, Okigaki M, Matsubara H. Replicative senescence of vascular smooth cells enhances the calcification through initiating the osteoblastic transition. J Physiol Heart Circ Physiol. 2009; 297:H1673–1684.
14. Zhu D, Mackenzie NCW, Millán JL, Farquharson C, MacRae VE. The Appearance and Modulation of Osteocyte Marker Expression during Calcification of Vascular Smooth Muscle Cells. PLoS ONE. 2011; 6:e19595. [PubMed: 21611184]
15. O'Neill WC, Sigrist MK, McIntyre CW. Plasma pyrophosphate and vascular calcification in chronic kidney disease. Nephrol Dial Transplant. 2010; 25:187–191. [PubMed: 19633093]
16. Narisawa S, Harmey D, Yadav MC, O'Neill WC, Hoylaerts MF, Millán JL. Novel inhibitors of alkaline phosphatase suppress vascular smooth muscle cell calcification. J Bone Miner Res. 2007; 22:1700–1710. [PubMed: 17638573]
17. Lomashvili KA, Garg P, Narisawa S, Millán JL, O'Neill WC. Upregulation of Alkaline Phosphatase and Pyrophosphate Hydrolysis: Potential Mechanism for Uremic Vascular Calcification. Kidney Int. 2008; 73:1024–1030. [PubMed: 18288101]
18. Villa-Bellosta R, Wang X, Millán JL, Dubyak GR, O'Neill WC. Extracellular pyrophosphate metabolism and calcification in vascular smooth muscle. Am J Physiol Heart Circ Physiol. 2011; 301:H61–H68. [PubMed: 21490328]
19. Hessle L, Johnson KA, Anderson HC, Narisawa S, Sali A, Goding JW, Terkeltaub R, Millán JL. Tissue non-specific alkaline phophatase and plasma membrane glycoprotein-1 are central antagonist regulators of bone mineralization. Proc Natl Acad Sci USA. 2002; 99:9445–9449. [PubMed: 12082181]
20. Harmey D, Hessle L, Narisawa S, Johnson KA, Terkeltaub R, Millán JL. Concerted regulation of inorganic pyrophosphate and osteopontin by Akp2, Enpp1, and Ank: an integrated model of the pathogenesis of mineralization disorders. Am J Pathol. 2004; 164:1199–1209. [PubMed: 15039209]
21. Houston B, Seawright E, Jefferies D, Hoogland E, Whitehead CC, Farquharson C. Identification and cloning of a novel phosphatase expressed at high levels in differentiating growth plate chondrocytes. Biochim Biophys Acta. 1999; 1448:500–506. [PubMed: 9990301]
22. Stewart AJ, Schmid R, Blindauer CA, Paisey SJ, Farquharson C. Comparative modeling of human PHOSPHO1 reveals a new group of phosphatases within the haloacid dehalogenase family. Protein Eng. 2003; 16:889–895. [PubMed: 14983068]
23. Houston B, Stewart AJ, Farquharson C. PHOSPHO1-a novel phosphatase specifically expressed at sites of mineralization in bone and cartilage. Bone. 2004; 34:629–637. [PubMed: 15050893]
24. Stewart AJ, Roberts SJ, Seawright E, Davey MG, Fleming RH, Farquharson C. The presence of PHOSPHO1 in matrix vesicles and its developmental expression prior to skeletal mineralization. Bone. 2006; 39:1000–1007. [PubMed: 16837257]
25. Roberts S, Narisawa S, Harmey D, Millán JL, Farquharson C. Functional involvement of PHOSPHO1 in matrix vesicle-mediated skeletal mineralization. J Bone Miner Res. 2007; 22:617–627. [PubMed: 17227223]
26. Roberts SJ, Stewart AJ, Sadler PJ, Farquharson C. Human PHOSPHO1 displays high specific phophoethanolamine and phosphocholine phosphatase activity. Biochem J. 2004; 382:59–65. [PubMed: 15175005]
27. Gremse DA. Lansoprazole: pharmacokinetics, pharmacodynamics and clinical use. Expert Opin Pharmaco-ther. 2001; 2:1663–1670.
28. Delomenede M, Buchet R, Mebarek S. Lansoprazole is an uncompetitive inhibitor of tissue-nonspecific alkaline phosphatase. Acta Biochim Polonica. 2009; 6:301–305.

29. MacRae VE, Davey MG, McTeir L, Narisawa S, Yadav MC, Millán JL, Farquharson C. Inhibition of PHOSPHO1 activity results in impaired skeletal mineralization during limb development of the chick. Bone. 2010; 46:1146–1155. [PubMed: 20053388]
30. Yadav MC, Simão AMS, Narisawa S, Huesa C, McKee MD, Farquharson C, Millán JL. Loss of skeletal mineralization by the simultaneous ablation of PHOSPHO1 and alkaline phosphatase function – A unified model of the mechanisms of initiation of skeletal calcification. J Bone Miner Res. 2011; 26:286–297. [PubMed: 20684022]
31. Huesa C, Yadav MC, Finnilä MJ, Goodyear SR, Robins SP, Tanner KE, Aspden RM, Millán JL, Farquharson C. PHOSPHO1 is essential for mechanically competent mineralization and the avoidance of spontaneous fractures. Bone. 2011; 48:1066–1074. [PubMed: 21272676]
32. Hsu HH, Camacho NP. Isolation of calcifiable vesicles from human atherosclerotic aortas. Atherosclerosis. 1999; 143:353–362. [PubMed: 10217364]
33. Kapustin AN, Davies JD, Reynolds JL, McNair R, Jones GT, Sidibe A, Schurgers LJ, Skepper JN, Proudfoot D, Mayr M, Shanahan CM. Calcium Regulates Key Components of Vascular Smooth Muscle Cell-Derived Matrix Vesicles to Enhance Mineralization. Circ Res. 2011; 109:e1–e12. [PubMed: 21566214]
34. Kozlenkov A, Hoylaerts MF, Ny T, LeDu MH, Millán JL. Residues determining the binding specificity of uncompetitive inhibitors to tissue-nonspecific alkaline phosphatase. J Bone Miner Res. 2004; 19:1862–1872. [PubMed: 15476587]
35. Dahl R, Sergienko E, Mostofi YS, Yang L, Ying Su Y, Simão AM, Narisawa S, Brown B, Mangravita-Novo A, Smith LH, O'Neill WC, Millán JL, Cosford NDP. Discovery and Validation of a Series of Aryl Sulfonamides as Selective Inhibitors of Tissue-Nonspecific Alkaline Phosphatase (TNAP). J Med Chem. 2009; 52:6919–6925. [PubMed: 19821572]
36. Jaroszewski L, Li Z, Cai XH, Weber C, Godzik A. FFAS server: novel features and applications. Nucleic Acids Res. 2011; 39:W38–44. [PubMed: 21715387]
37. Roy A, Kucukural A, Zhang Y. I-TASSER: a unified platform for automated protein structure and function prediction. Nat Protoc. 2010; 5:725–738. [PubMed: 20360767]
38. Schwede T, Kopp J, Guex N, Peitsch MC. SWISS-MODEL: An automated protein homology-modeling server. Nucleic Acids Res. 2003; 31:3381–3385. [PubMed: 12824332]
39. Grosdidier A, Zoete V, Michielin O. SwissDock a protein-small molecule docking web service based on EADock DSS. Nucleic Acids Res. 2011; 39:W270–277. [PubMed: 21624888]
40. Grosdidier A, Zoete V, Michielin O. Fast docking using the CHARMM force field with EADock DSS. J Comput Chem. 2011 May 3.10.1002/jcc.21797
41. MacKerell AD Jr, Banavali N, Foloppe N. Development and current status of the CHARMM force field for nucleic acids. Biopolymers. 2000; 56:257–265. [PubMed: 11754339]
42. Ciancaglini P, Yadav MC, Simão AM, Narisawa S, Pizauro JM, Farquharson C, Hoylaerts MF, Millán JL. Kinetic analysis of substrate utilization by native and TNAP-, NPP1-, or PHOSPHO1-deficient matrix vesicles. J Bone Miner Res. 2010; 25:716–723. [PubMed: 19874193]
43. Towler DA. Vascular calcification: a perspective on an imminent disease epidemic. IBMS BoneKEy. 2008; 5(2):41–58.
44. Fleisch H, Schibler D, Maerki J, Frossard I. Inhibition of aortic calcification by means of pyrophosphate and polyphosphates. Nature. 1965; 207(5003):1300–1301. [PubMed: 4287147]
45. Markello TC, Pak LK, Hilaire CSt, Dorward H, Ziegler SG, Chen MY, Chaganti K, Nussbaum RL, Boehm M, Gahl WA. Vascular pathology of medial arterial calcification in NT5E deficiency: Implications for the role of adenosine in pseudoxanthoma elasticum. Mol Genet Metab. 2011; 103(1):44–45. [PubMed: 21371928]
46. Sidique S, Ardecky R, Su Y, Narisawa S, Brown B, Millán JL, Sergienko E, Cosford NDP. Design and synthesis of pyrazole derivatives as potent and selective inhibitors of tissue-nonspecific alkaline phosphatase (TNAP). Bioorg Med Chem Lett. 2009; 19:222–225. [PubMed: 19038545]
47. Sergienko E, Su Y, Chan X, Brown B, Hurder A, Narisawa S, Millán JL. Identification and characterization of novel tissue-nonspecific alkaline phosphatase inhibitors with diverse modes of action. J Biomol Screen. 2009; 14(7):824–837. [PubMed: 19556612]

48. Chung TD, Sergienko E, Millán JL. Assay format as a critical success factor for identification of novel inhibitor chemotypes of tissue-nonspecific alkaline phosphatase from high-throughput screening. Molecules. 2010; 15(5):3010–3037. Review. [PubMed: 20657462]

49. Sergienko EA, Millán JL. High-throughput screening of tissue-nonspecific alkaline phosphatase for identification of effectors with diverse modes of action. Nat Protoc. 2010; 5(8):1431–1439. [PubMed: 20671726]

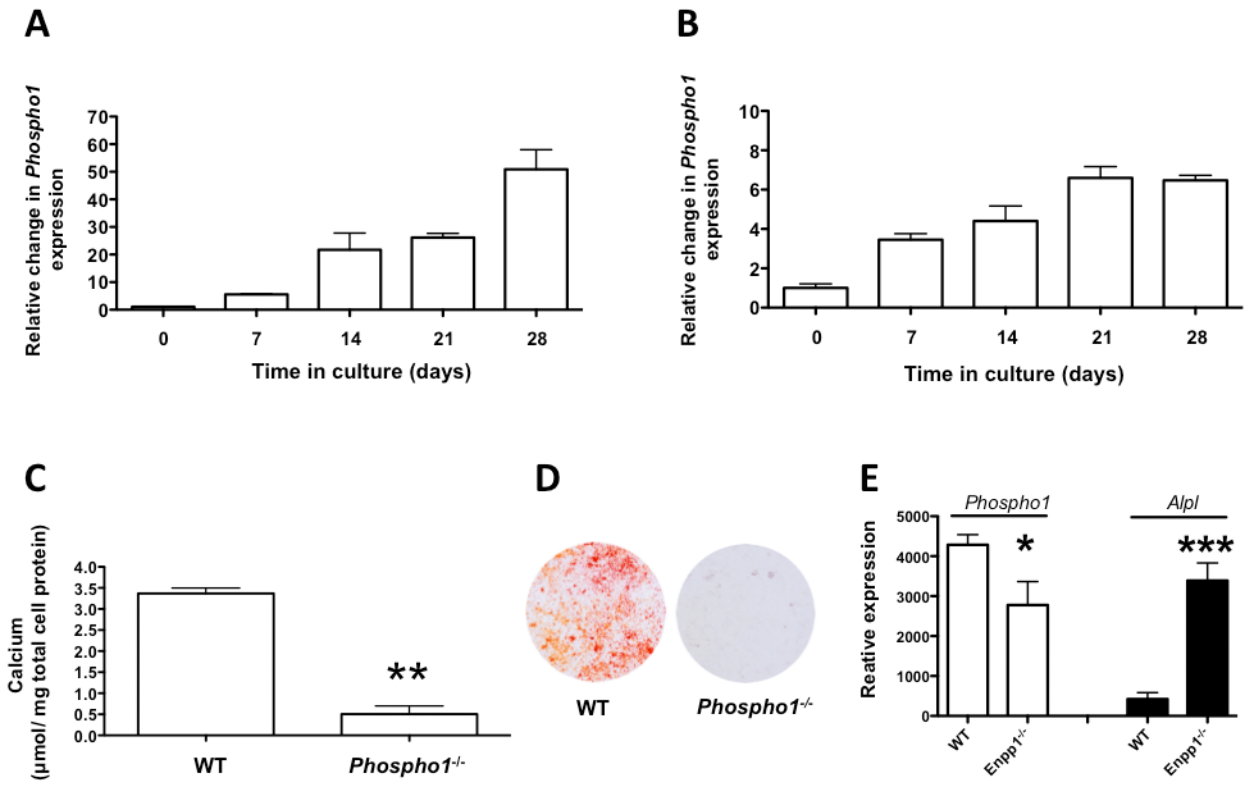

Fig. 1. Expression of *Phospho1* in VSMCs and its role in VSMC mineralization

Normalized *Phospho1* mRNA expression as a function of the calcification time in cultured WT murine (**A**) calvarial osteoblasts and (**B**) aortic VSMCs. (**C**) Calcium deposition in WT and *Phospho1*$^{-/-}$ murine aortic VSMCs after 28 days of culture. (**D**) Alizarin Red staining of WT and *Phospho1*$^{-/-}$ murine aortic VSMCs after 28 days of culture. (**E**) Normalized *Phospho1* and *Alpl* expression in *Enpp1*$^{-/-}$ aortic VSMCs versus WT VSMCs, after 21 days in culture under mineralizing conditions. Results are presented as mean ± S.E.M. (*$p < 0.05$, **$p < 0.01$, ***$p < 0.001$).

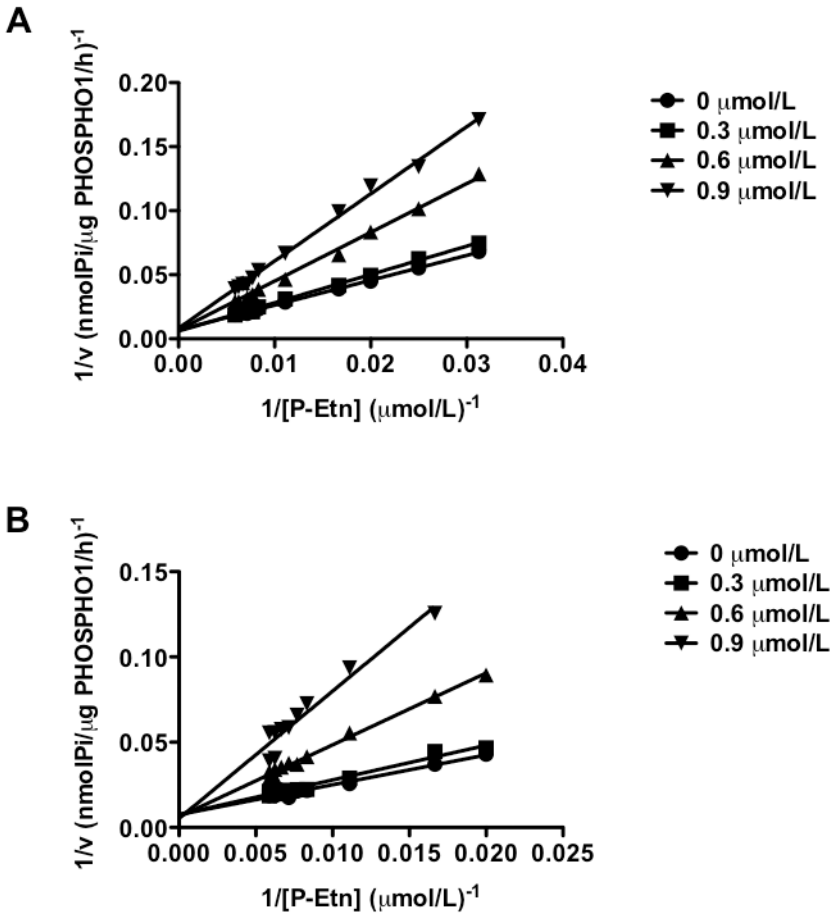

Fig. 2. Mode of action of PHOSPHO1 inhibition by lansoprazole and MLS-0263839

Double reciprocal plots of PHOSPHO1 activity versus the concentration of the PHOSPHO1 substrate P-Etn (32 – 170 μmol/L), in the presence of increasing concentrations of lansoprazole (A) and MLS-0263839 (B). Results are presented as mean ± S.E.M.

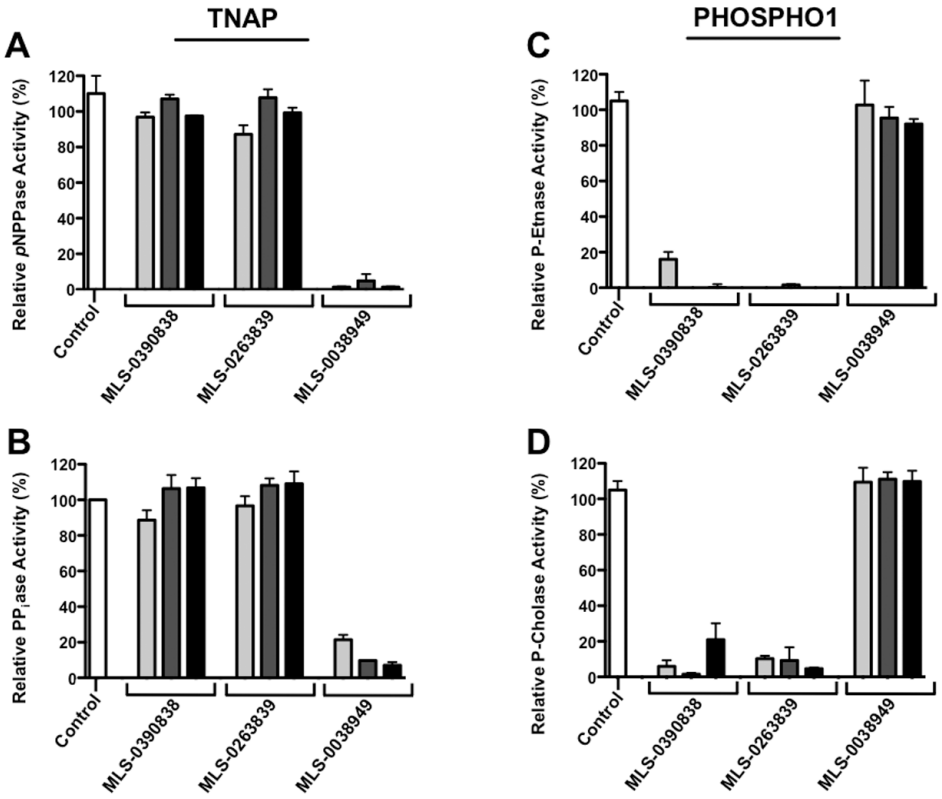

Fig. 3. Selectivity of PHOSPHO1 and TNAP inhibitors

Point experiments with the PHOSPHO1 inhibitors MLS-0390838 and MLS-0263939 and TNAP inhibitor MLS-0038949 at 0 (100% control, open bar), 1 (light gray bars), 10 (dark gray bars) and 30 (black bars) μmol/L, illustrating specificity during hydrolysis by TNAP of the substrates pNPP (**A**, 10 mmol/L Pnpp in 50 mmol/L Tris-HCl buffer, pH 7.5, containing 1 mmol/L $MgCl_2$, 20 μmol/L zinc acetate) and PP_i (**B**, 60 μmol/L PP_i in 50 mmol/L Tris-HCl buffer, pH 7.5, containing 1 mmol/L $MgCl_2$, 20 μmol/L ZnAc), and by PHOSPHO1 for the substrates P-Etn (**C**, 62.5 μmol/L P-Etn in 20 mmol/L MES-NaOH, pH 6.7, 0.01% (w/v) BSA, 0.0125% (v/v) Tween 20, 2 mmol/L $MgCl_2$) and P-Cho (**D**, 62.5 μmol/L P-Cho in MES-NaOH, pH 6.7, 0.01% (w/v) BSA, 0.0125% (v/v) Tween 20, 2 mmol/L $MgCl_2$).

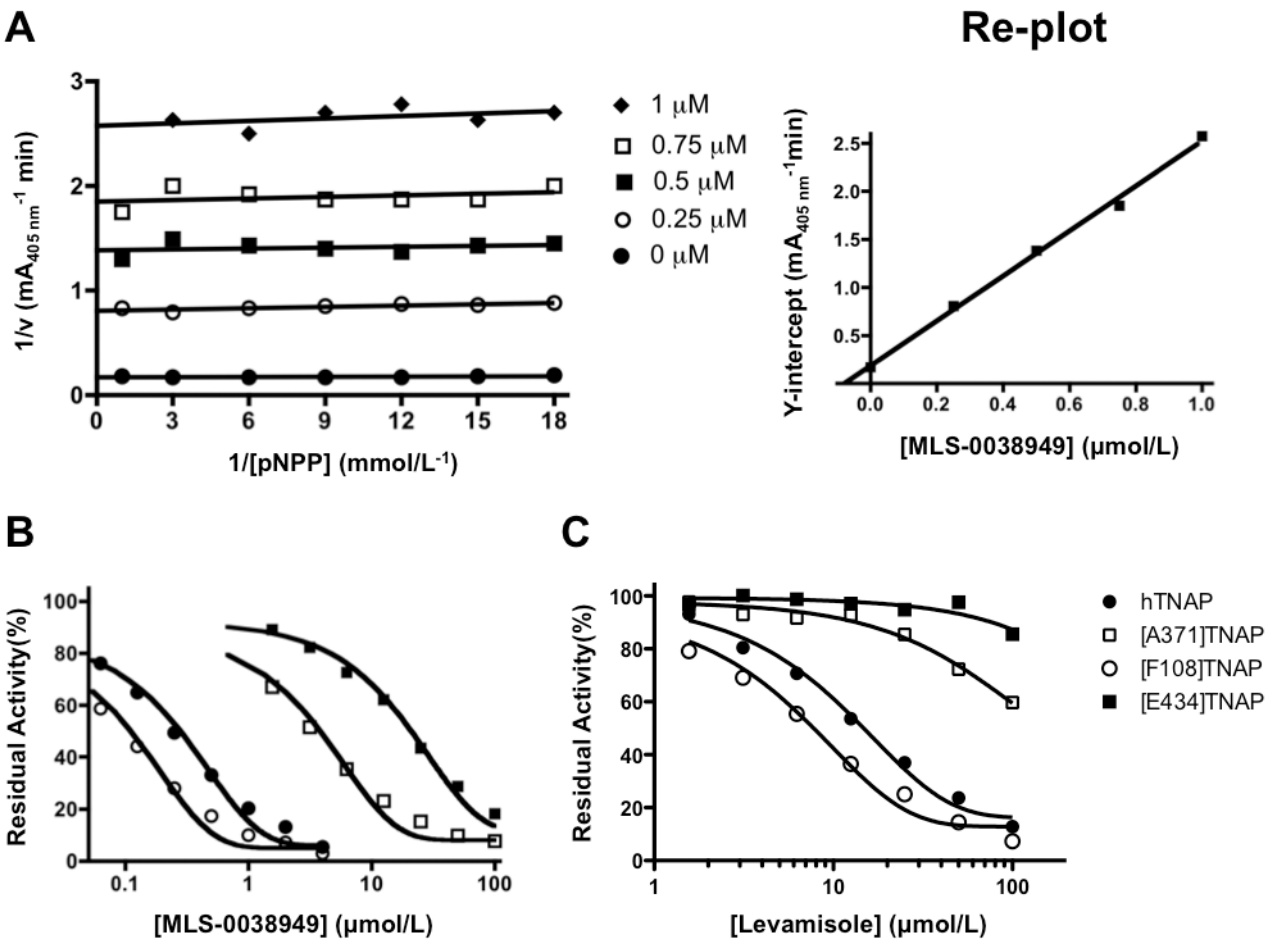

Fig. 4. Mode of action of TNAP inhibition by MLS-0038949

Double reciprocal plots of TNAP activity versus the concentration of the TNAP substrate pNPP (0.055 – 1 mmol/L) at pH 7.4, in the presence of increasing concentrations of MLS-0038949 and re-plot of the y-intercepts versus the concentration of MLS-0038949 (A). Residual TNAP activity during dose-dependent inhibition by MLS-0038949 (B) and levamisole (C) of hTNAP and its three active site mutants (Tyr371Ala, Glu108Phe and His434Glu).

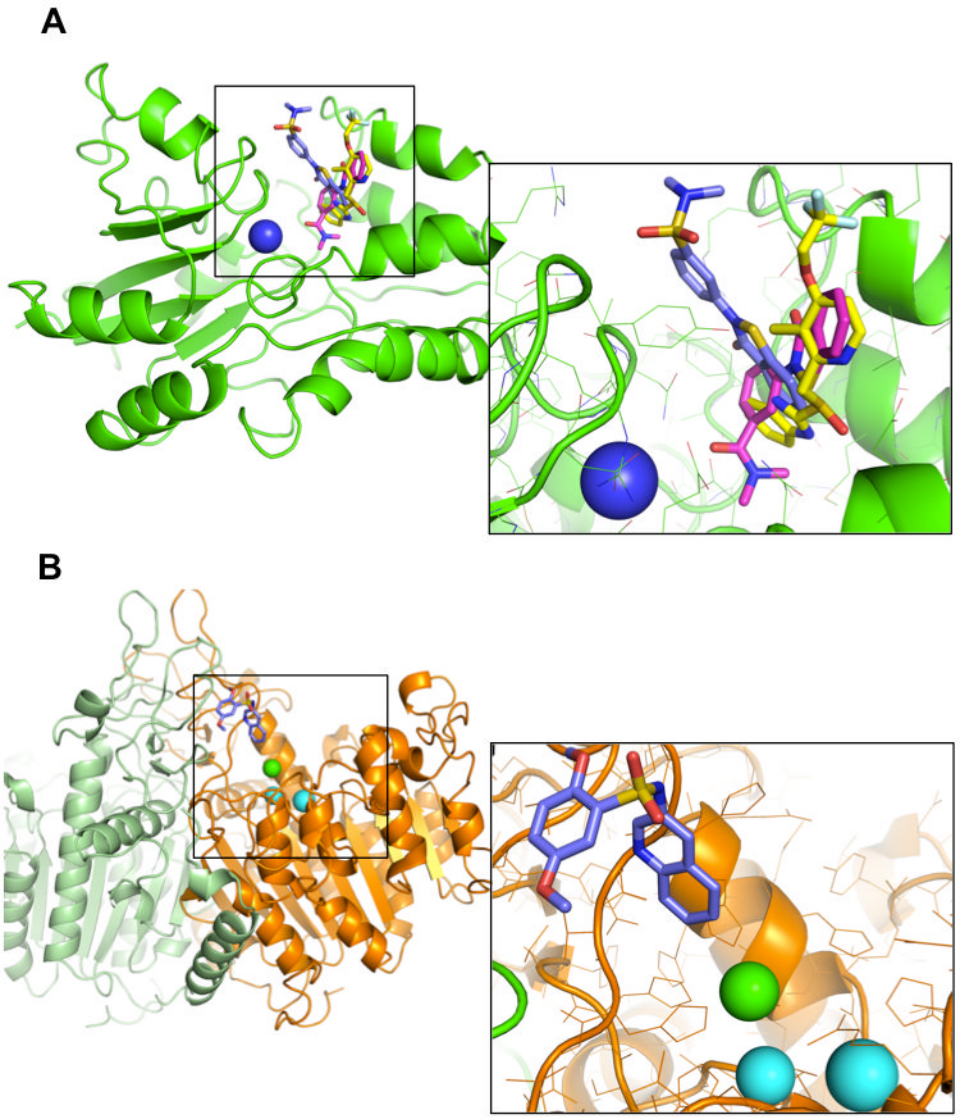

Fig. 5. Modeling of docked PHOSPHO1 and TNAP inhibitors

Computer docking of PHOSPHO1 inhibitors MLS-0263839 (in blue) and MLS-0390838 (in purple) in comparison to lansoprazole (in yellow) into the active site of the modeled structure of PHOSPHO1 (**A**) and of the potent uncompetitive TNAP inhibitor MLS-0038949 (in blue) in the active site of the modeled structure of TNAP (**B**). Insets: close-up views of binding inhibitors.

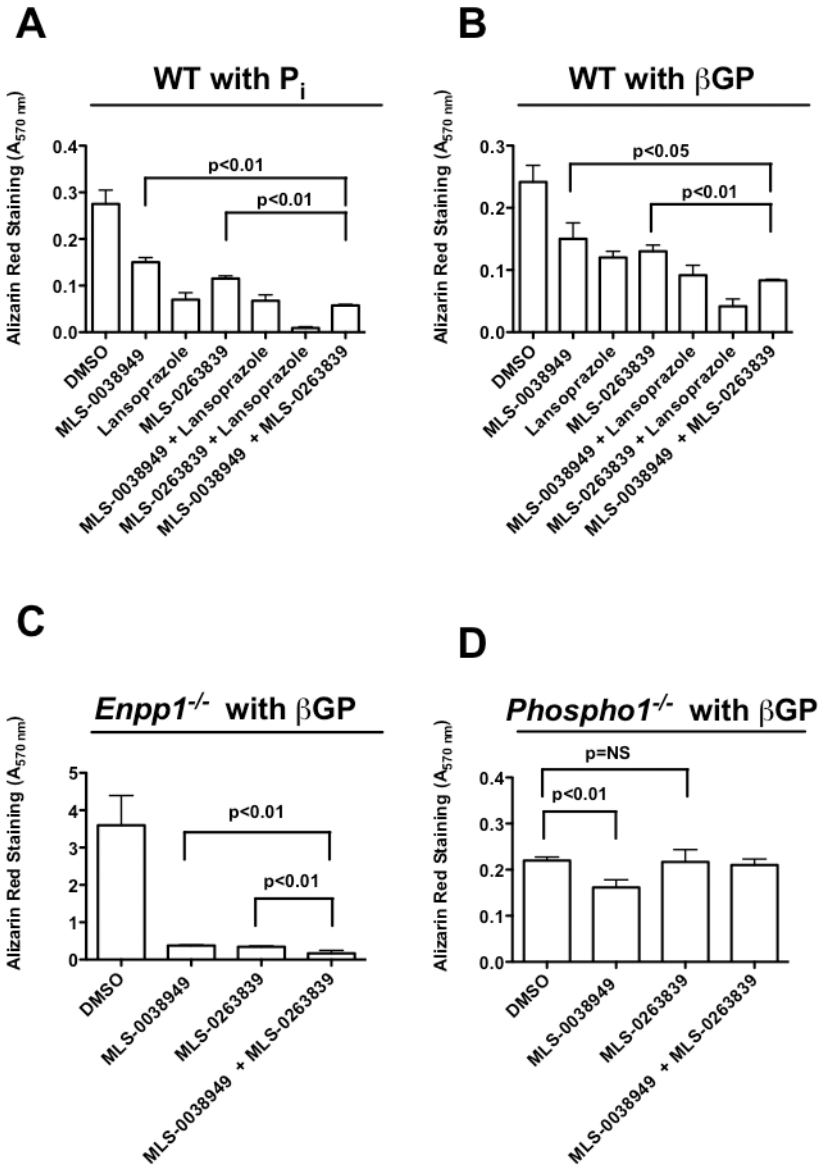

Fig. 6. Inhibition of matrix mineralization

Alizarin Red-staining ($A_{570\ nm}$) of 21 day cultures of WT VSMC in the presence of inorganic phosphate (A) and in the presence of β-glycerophosphate for WT (**B**), *Enpp1*$^{-/-}$ (**C**) and *Phospho1*$^{-/-}$ (**D**) VSMCs. The cells were cultured with 30 μmol/L of the TNAP inhibitor MLS-0038949 and the PHOSPHO1 inhibitors lansoprazole and MLS-0263839, either alone or combined, as indicated. Calcium deposition in 21-day VSMC cultures was evaluated by staining cell layers with Alizarin Red.

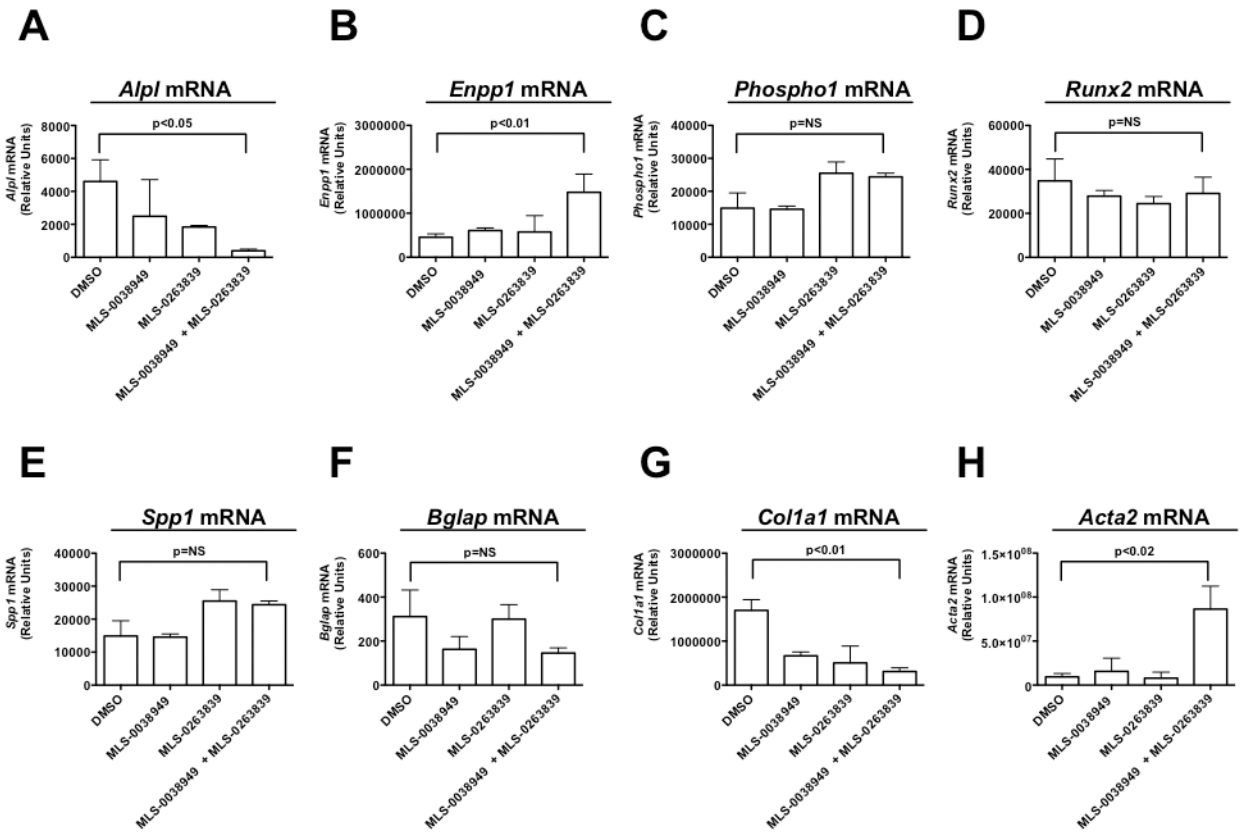

Fig. 7. Gene expression changes in WT VSMCs treated with inhibitors

WT VSMCs were cultured for 21 days in the presence of TNAP inhibitor MLS-0038949 or PHOSPHO1 inhibitor MLS-0263839, either alone or combination, as indicated. The mRNA expression was determined by qPCR for *Alpl* (**A**), *Ennp1* (**B**), *Phospho1* (**C**), *Runx2* (**D**), *Spp1* (**E**), *Bglap* (**F**), *Col1a1* (**G**), and *Acta2* (**H**).

Table

IC_{50} values for PHOSPHO1 inhibitors, using the physiological substrates P-Etn and Pcho.

Compound	P-Etn IC_{50} (μmol/L)	P-Cho IC_{50} (μmol/L)
MLS-0437435.001	1.90 ± 0.15	1.98 ± 0.30
MLS-0437436.001	0.39 ± 0.04	0.49 ± 0.05
MLS-0437437.001	11.20 ± 1.20	10.50 ±0.60
MLS-0437438.001	5.90 ±0.08	4.10 ±0.03
MLS-0437439.001	0.90 ±0.15	0.60 ±0.12
MLS-0390837	1.20 ±0.19	1.20 ±0.17
MLS-0390838	0.13 ±0.01	0.16 ±0.02
MLS-0263839	0.14 ± 0.03	0.24 ± 0.06
MLS-0315922	0.20 ± 0.01	0.24 ± 0.02
Lansoprazole	0.07 ± 0.01	0.06 ± 0.01